microplastics

MDPI

Article

Exploring Uptake of Toxic Environmental Pollutants onto Commercial Microplastics: An Insight of Thermodynamic Predictive Scenarios, Kinetics and Influencing Factors

Domenica Mosca Angelucci [1], Marco Manetti [1], Enrica Donati [2,*] and Maria Concetta Tomei [1,*]

[1] Water Research Institute, National Research Council (CNR-IRSA), Via Salaria km 29.300, CP 10, Monterotondo Stazione, 00015 Rome, Italy; domenica.mosca@irsa.cnr.it (D.M.A.); marco.manetti@irsa.cnr.it (M.M.)
[2] Institute for Biological Systems, National Research Council (CNR-ISB), Via Salaria km 29.300, CP 10, Monterotondo Stazione, 00015 Rome, Italy
* Correspondence: enrica.donati@cnr.it (E.D.); concetta.tomei@irsa.cnr.it (M.C.T.)

Abstract

This study investigates the sorption process of selected pollutants, namely naphthalene (NAP), pentachlorophenol (PCP), sulfamethoxazole (SMX), and ibuprofen (IBU), onto different real microplastics (MPs) under controlled laboratory conditions. Sorption tests reveal variable affinities depending on the chemical and physical interactions between polymers and pollutants. NAP showed the greatest uptake on the majority of tested MPs, followed by PCP and SMX, while IBU exhibited negligible sorption. Kinetic tests indicate a general rapid initial uptake, followed by lower sorption rates leading to equilibrium within days. Theoretical thermodynamic affinity estimations, based on the Hansen solubility parameter (HSP) method, previously tested only on antibiotics, are applied for the first time to commercial MPs and several pollutant categories such as PAHs, pesticides and other pharmaceuticals. Predictions have been validated with experimental results and generally show very good agreement with the affinity ranking derived by experimental data. However, some limitations occur due to the heterogeneity of the real MPs and different environmental conditions. Factors affecting, to different extents, MPs' uptake include hydrophobicity and electrostatic forces, as well as pH and particle size. This work advances understanding of MPs' role as vectors of pollutants in aquatic environments and validates the use of an innovative combined experimental–theoretical approach useful as a tool to predict associated risk.

Keywords: microplastics; organic contaminants; thermodynamic predictive model; sorption kinetics; Hansen solubility parameters; contamination diffusion

Academic Editor: Juan A. Conesa

Received: 11 November 2025
Revised: 31 March 2026
Accepted: 16 April 2026
Published: 1 May 2026

1. Introduction

In recent years, a growing concern has been raised on the impact of microplastics (MPs) on ecosystems, particularly within aquatic environments. MPs are defined as particles smaller than 5 mm that can be either intentionally manufactured at a microscale (*primary*) or originated from the degradation of larger plastic products (*secondary*) [1]. They are easily transported in water, especially low-density particles [2], and can accumulate in aquatic organisms, entering the food chain [3]. While MPs have been proven to be inherently toxic to organisms [3,4], they can also sorb and transport other pollutants occurring in aquatic environments, thereby increasing their overall hazard potential [5].

Investigating the uptake interactions between MPs and other pollutants is essential to advance the knowledge on how MPs influence the fate, transport, and ecological impacts of contaminants. Indeed, sorption of organic pollutants by MPs has been deeply investigated in recent years to highlight driving mechanisms of sorption processes related to MPs' physical and chemical characteristics, contaminant intrinsic properties and environmental conditions and to develop process models. This last point is one of the most challenging, timely, and relevant among specialized literature topics [6]. For instance, prediction of sorption behavior may be difficult given the complexity of process mechanisms and the number of impacting factors. To this aim, two main approaches can be identified in the literature, i.e., mechanistic methods (for both kinetic and equilibrium predictions) and predictive methods based on thermodynamic descriptors [7,8]. The former approach for the kinetic models involves empirical equations, such as pseudo-first order (PFO) and pseudo-second order (PSO) equations, and isotherms such as Freundlich or Langmuir expressions to predict the equilibrium conditions. One of the main limitations of these models is that they are based on empirically derived parametrization [9], and thus they may have limited ability to capture complex interactions.

An alternative approach is the theoretical estimation of thermodynamic affinity between sorbent or extractant medium (i.e., MPs) and solutes, such as organic pollutants. Among the proposed procedures, the Hansen solubility parameter (HSP) method [10] has been successfully applied to evaluate polymer–solute interactions [11–13] and offers a powerful tool to predict the interaction behavior of different MP–contaminant pairs [14]. To the best of our knowledge, previous applications of the HSP method on MPs have been only focused on the sorption of antibiotics (ciprofloxacin and amoxicillin) by polyethylene terephthalate (PET) [15,16].

The aim of this work is to offer an insight into sorption processes of common organic pollutants onto MPs originating from commercial plastic products through experimental tests and process modeling. MPs typically employed in experiments are usually bought specifically for the purpose, and only a few investigations have been carried out so far using commercial plastic products or MPs taken from real environments [17]. While the use of pristine materials allows result reproducibility operating with well-defined MP characteristics, it is less representative of real conditions. This is because MPs in aquatic environments mostly originate from the fragmentation and degradation of used plastic products [18]. In contrast to the majority of studies employing pristine laboratory-prepared polymers, MPs obtained from commercial plastic products, which more realistically reflect the materials found in natural environments, have been used in this study. Seven plastic materials have been selected, i.e., high-density polyethylene (HDPE), low-density polyethylene (LDPE), polyamide (PA), PET, polypropylene (PP), polystyrene (PS) and polyvinyl chloride (PVC), to cover widespread plastic products. Indeed, these polymers represent almost 70% of European plastic production in 2023 according to the last report of Plastics Europe in 2024 [19]. Target organic contaminants including naphthalene (NAP), pentachlorophenol (PCP), ibuprofen (IBU) and sulfamethoxazole (SMX) were selected to represent four classes of commonly detected environmental contaminant categories [20,21], i.e., polycyclic aromatic hydrocarbons (PAHs), pesticides, pharmaceuticals and antibiotics.

Sorption experiments have been carried out to characterize the uptake of target pollutants on selected MPs by considering thermodynamics (i.e., equilibrium data) and process kinetics. Results were achieved with an innovative approach, combining thermodynamic prediction and experimental validation and provide an additional contribution to the present state of knowledge on the processes governing pollutant–MP interactions. Moreover, the HSP method, applied in this study for the first time to a wide range of commercial MPs and pollutant categories, is demonstrated to be a valid methodology to define the role

of MPs as contamination vectors. This strategy can also be a propaedeutic tool for evaluating the risk assessment derived from the environmental diffusion of different pollutants sorbed onto MPs.

2. Materials and Methods

2.1. MPs and Chemicals

Commercial plastic products (e.g., disposable water bottles, containers and food trays, labware, cable ties, etc.) of HDPE, LDPE, PA, PET, PP, PS, PVC have been collected (Figure S1a) and prepared for the experimentation as described below.

NAP (CAS n. 91-20-3, purity > 99%), PCP (CAS n. 87-86-5, purity > 99%), IBU (as sodium salt ibuprofen, CAS n. 31121-93-4, purity > 98%) and SMX (CAS n. 723-46-6, purity > 98%) were all supplied by Sigma Aldrich (St. Louis, MO, USA). Methanol, acetonitrile and water (all HPLC grade) were bought from VWR International S.r.l. (Milan, Italy). Formic acid was purchased from Carlo Erba (Milan, Italy). Minisart NY filters (nylon membrane, 15 mm × 0.2 µm) were obtained from Sartorius (Göttingen, Germany). Other reagents employed for experiments, i.e., HCl and NaOH for pH control as well as acetone for MP preparation, were commercial grade and also provided by Sigma Aldrich (USA).

2.2. MP Preparation

MP debris were obtained by cutting or grating commercial products using a fine shredder or food processor [22,23], as shown in Figure S1b–d. The obtained plastic debris were firstly sieved through a 5 mm sieve to eliminate larger particles, then washed with acetone for 20 min to remove previous impurities. Then, particle size distribution (PSD) was assessed for each polymer as described below. Subsequently, the MP debris were washed again to eliminate impurities originated from sieving procedures with two subsequent cleaning steps of 20 min each with (i) 1:1 deionized water–methanol solution and (ii) only deionized water. At the end of the washing procedure, MPs were oven-dried at 40 °C for 24 h and stored in sealed glass flasks at room temperature until use for additional characterization and testing.

2.3. MP Characterization

Characterization of MP particles included PSD, Fourier transform infrared (FT–IR) and X-ray diffraction (XRD) analysis. PSD was characterized with an electromechanical sieve by using stacks of stainless sieves with meshes of 0.5, 1, 1.7, 2.8 and 5 mm. For each sample, a known amount of plastic (around 20 g) was placed in the stack and shaken for 15 min. Fractions of different sizes were weighed and then gathered to be utilized in the following experiments.

FT–IR spectra were acquired using an IR Prestige-21 spectrometer (Shimadzu Europa GmbH, Düsseldorf, Germany) equipped with an attenuated total reflectance (ATR) module. The measurements were carried out in the 400–4000-cm^{-1} range by dint of a ZnSe crystal with a resolution of 4 cm^{-1} and 32 scans at room temperature. A break in the range 1800–2500 cm^{-1} of the spectra is included to exclude the environmental CO_2 noise.

XRD analyses were carried out with a Rigaku Smartlab SE (Rigaku, Tokyo, Japan) diffractometer operating with a Cu Kα radiation anode at 40 kV and 30 mA and equipped with a silicon strip Rigaku D/teX Ultra 250 detector (Rigaku, Tokyo, Japan). Data were collected over the 2θ range of 5–80° at a rate of 1° min^{-1} and with a 0.1° step resolution. XRD data were also qualitatively analyzed through SmartLab Studio II software (x54v4.6.426.0 version, Rigaku, Tokyo, Japan), based on the use of the free POW_COD database [24].

2.4. Sorption Tests

Sorption tests were performed in a thermostatic (20 °C) dark room by using 15 mL glass vials continuously shaken at 25 rpm by a rotary tube stirrer (F205 G, Falc Instruments s.r.l., Bergamo, Italy). For each sorption trial (carried out in duplicate), 1 g/L of MP was added to the target pollutant solution (12.5 mL, 5 mg/L, pH 7), then the vial was closed and vigorously manually shaken to ensure the wettability of MPs, covered with aluminum papers and put into the shaker. The stirrer provides continuous 360° rotation of the tubes, ensuring continuous mixing of the liquid phase and particles during the experiments. Control experiments were conducted in parallel under identical experimental conditions and sampled at the same points of sorption tests, as follows:

- Control_1: MPs + water blanks without target contaminants to address the potential influence of additives or leachates from commercial plastics on the UV–Vis measurements;
- Control_2: target contaminant solution without MP addition to assess potential contaminant losses unrelated to sorption (e.g., adsorption to glassware, volatilization, or degradation).

Duplicate vials have been removed from the experimental run at different times (between 1 and 12 days) for each MP–target contaminant pair and final liquid concentration of the target contaminant was analyzed to determine the sorption capacity ($q_{MP,t}$ mg/g), calculated according to the following mass balance (Equation (1)):

$$q_{MP,t} = \frac{(C_{w,0} - C_{w,t})}{w_{MP}} \cdot V_w \quad (1)$$

where $C_{w,0}$ and $C_{w,t}$ are, respectively, the water concentrations of the target compound at initial time (corrected by control tests, when necessary, as suggested by Wang and Wang [25]) and at time t, w_{MP} and V_w are the MP weight and liquid volume, respectively.

For some cases, duration of sorption tests has been prolonged depending on the time required to reach the equilibrium conditions (defined t_{eq}). This condition has been verified when the variation in the liquid-phase concentration between at least two subsequent sampling points (conducted at time interval of 2–3 days) was lower than 5%, evaluated as the relative standard deviation (RSD) of the measured concentrations in the aqueous phases. Based on this criterion, t_{eq} was evaluated for each MP–contaminant pair as the first sampling point satisfying the abovementioned condition.

Operating conditions were carefully chosen to balance the need to reproduce real environmental conditions and laboratory-imposed limitations: tested mixing speed (i.e., 25 rpm) was as low as possible to be closer to the field conditions of surface water environments. Moreover, regarding MP and contaminant concentrations, average values of 1 g/L and 5 mg/L were selected, respectively, with reference to literature values. Indeed, Table S1 gives an overview of previous studies on sorption of NAP, PCP, IBU and SMX onto different MPs: reported ranges of MP and target compound concentrations are 0.05–50 g/L and 0.02–20 mg/L [26–39].

Additional tests at pH 4 have been performed for SMX.

The uptake of each target pollutant by MPs has been calculated according to the following Equation (2):

$$\text{Uptake}(\%) = \frac{q_{MP,e} \cdot w_{MP}}{C_{w,0} \cdot V_w} \cdot 100 \quad (2)$$

where $q_{MP,e}$ is the equilibrium polymeric concentration (average of all equilibrium concentrations).

Equilibrium data for both polymeric and liquid concentrations have also been employed to estimate the partition coefficients (PCs) for each MP–contaminant pair according to the following Equation (3):

$$PC = \frac{q_{MP,e}}{C_{w,e}} \quad (3)$$

2.5. Analysis

Quantification of target pollutants in filtered (Whatman, 0.2 µm nylon, Sigma-Aldrich, St. Louis, MO, USA) liquid samples has been performed with two analytical approaches: NAP and PCP were measured using a UV–visible spectrophotometer (PerkinElmer Lambda 25, Waltham, MA, USA), according to procedures adapted from previous works on NAP [40,41] and PCP [42,43]. Pharmaceuticals IBU and SMX were quantified using a UPLC-PDA method.

Regarding spectrophotometric analysis, absorption spectra were recorded in the range of 200–800 nm at 1 nm intervals for both compounds. The maximum absorption wavelengths identified and used to determine NAP and PCP concentrations were 276 and 320 nm, respectively. Calibration standard solutions were used to create calibration curves for each compound (n = 6). The solutions were in the range of 0.815–10 for NAP and 0.335–10 mg/L for PCP.

Determination of IBU and SMX in aqueous samples was obtained by an Acquity™ H-Class Bio UPLC system (Waters, Milford, MA, USA) comprising an autosampler, a thermostatically controlled column, a PDA detector and an Empower™ 3 workstation for processing acquired data. An Acquity UPLC BEH C18 column (50 mm × 2.1 mm id, 1.7 µm), equipped with an Acquity UPLC BEH C18 pre-column (5 mm × 2.1 mm id, 1.7 µm), both from Waters (Milford, MA, USA), were used to carry out chromatographic analyses. Table S2 reports the column temperature, the mobile phases employed for analyte elution in isocratic mode, and the wavelengths used for IBU and SMX detection.

Calibration curves were achieved by analyzing standard solutions for each compound of various concentrations (n = 6) in triplicate within the following concentration ranges: IBU 0.0464–7.5 mg/L, SMX 0.0102–7.00 mg/L.

Both analytical methods were validated in terms of linearity, sensitivity and precision, as deeply described in Section S2 of the Supplementary Material.

2.6. Kinetic Modeling

The kinetics data have been correlated with both PFO and PSO kinetic models, according to the following equations (Equations (4) and (5)):

$$\frac{dq_{MP,t}}{dt} = K_1\left(q_{MP,e} - q_{MP,t}\right) \quad (4)$$

$$\frac{dq_{MP,t}}{dt} = K_2\left(q_{MP,e} - q_{MP,t}\right)^2 \quad (5)$$

where $q_{MP,t}$ (mg/g) is the sorption capacity at time t and K_1 (1/d) and K_2 (g/mg d) are the rate constants of PFO and PSO models, respectively. For both models, initial conditions of $q_{MP,0} \rightarrow 0$ for $t \rightarrow 0$ have been applied and $q_{MP,e}$ and K_i were obtained for each model.

The Scientist 3.0 software package (Micromath, Salt Lake City, UT, USA) has been employed for data fitting of kinetic tests and the estimation of best parameters by applying the differential form of both kinetic equations. Goodness of fit was evaluated with R^2, coefficient of determination (CD) and the sum of squared errors (SSE).

3. Predictive Thermodynamic Method

The theory based on the solubility parameters can be applied to predict the nature and magnitude of the interactions between different compounds and/or materials. Hildebrand and Scott [44] proposed a basic method to evaluate thermodynamic affinity using the principle of "*like attracts like*," based on binary solute–solvent interactions quantified by Hildebrand solubility parameters (δ), which reflect a solvent's relative capability to dissolve a given solute. Nevertheless, this approach focuses on binary interactions, not considering the differentiation of interaction types, which reduces prediction accuracy for highly polar compounds. Hansen introduced a cumulative solubility parameter (δ_{HSP}) that distinguishes three types of molecular interactions: non-polar (dispersion forces), polarizable (dipole–dipole interactions), and hydrogen bonding [10]. This parameter can be evaluated by the combination of the dispersive (δ_D), polar (δ_P), and hydrogen-bonding (δ_H) solubility data according to the following expression (Equation (6)).

$$\delta_{HSP} = \sqrt{\left(\delta_D^2 + {\delta_P}^2 + {\delta_H}^2\right)} \quad (6)$$

This approach, originally developed for solvent–solute interaction, can be extended to polymers [45] and provides a robust framework for assessing the sorption interactions between polymers and pollutants. Closer δ_{HSP} values between a polymer and a solute indicate higher molecular similarity and thus higher affinity. Moreover, solubility parameters of both polymer and compound can be combined to estimate Ra distance between these two components according to Equation (7).

$$Ra = \sqrt{\left[4\cdot\left(\delta_{D,p} - \delta_{D,c}\right)^2 + \left(\delta_{P,p} - \delta_{P,c}\right)^2 + \left(\delta_{H,p} - \delta_{H,c}\right)^2\right]} \quad (7)$$

where the subscripts *p* and *c* indicate the polymer and the compound, respectively. The smaller the Ra "distance" between polymer and compound, the greater the thermodynamic affinity and higher likelihood of interaction.

Data for each tested polymer and compound were collected (Table S3) to evaluate the potentialities of HSPs for predicting sorption scenarios [10,46,47].

4. Results and Discussion

4.1. MP Characterization

Results of PSD characterization of MPs tested in this study are reported in Figure S2 and Table S4. Granulometric data identify PA and PVC as the MPs characterized by the highest content of smaller fractions, with more than 94% and 99% of particles < 2.8 mm, respectively, while for other MPs, this percentage ranged from 48% (PS) to 85% (HDPE). A more detailed analysis of the particle size distribution shows that the fraction < 1 mm ranged from 2.5% (PA) to 22.2% (PP), whereas the 1–1.7 mm fraction varied between 10.8% (PS) and 52.0% (PVC). The 1.7–2.8 mm fraction was predominant for several MPs, particularly PA (72.7%) and LDPE (58.8%), as reported in Table S4. Although the particle size plays a relatively minor role compared to other physical parameters, it can still influence the sorption capacity and rate and the time required to reach equilibrium conditions [48]. In general, both adsorption capacity and rate increased as the particle size decreased, i.e., surface area increased. Surface area can vary depending on the particle shape, pores and cracks of plastic debris induced by weathering, aging or biodegradation of the plastics themselves.

XRD analysis has been performed to characterize the crystalline structure of the tested MPs and to support the interpretation of their interaction with target pollutants. XRD spectra are shown in Figure S3: well-defined diffraction peaks were observed for most MP

samples (HDPE, LDPE, PA, PP, and PET), confirming their semicrystalline nature [49–51], while PS and PVC were found to be predominantly amorphous. In addition, the diffractograms of PS and PVC (Figure S3f and Figure S3g, respectively) were dominated by sharp reflections attributable to an inorganic filler, probably calcium carbonate ($CaCO_3$), commonly used in commercial plastics to enhance the toughness of the polymer matrix [52,53]. A detailed analysis of XRD spectra is provided in the Supplementary Material (Section S1).

FT-IR characterization was employed to identify the composition of MP samples and to provide information regarding functional groups potentially involved in pollutant uptake. FT-IR spectra are shown in Figure S4 and a detailed description for each MP sample is given in the Supplementary Material (Section S1). Overall, FT-IR analysis confirms the identity of all investigated polymers [54–62] and reveals the presence of oxidation products for PVC (Figure S4g) and, to a minor extent, for HDPE and LDPE (Figure S4a,b), probably due to aging processes [63]. This finding is consistent with the use of MP samples obtained from used consumer products, which likely experienced aging and oxidative degradation prior to testing.

4.2. Sorption Tests

4.2.1. Uptake Evaluation

Time profiles of liquid concentrations obtained from sorption tests are reported in Figure S5 while Figures 1–3 show the polymeric concentration profiles for NAP, PCP and SMX, respectively. Moreover, results of control tests are reported in Figure S6 and discussed in Section S3 of the Supplementary Material. NAP is the sole compound sorbed by all the tested polymers, followed by PCP, which was retained by HDPE, LDPE, PP and PA, and then SMX sorbed only by PA, PS and PVC. IBU was the only pollutant for which no significant sorption has been detected in the operating conditions tested in this study (Figure S5c).

Uptake values were within the ranges of 4–67%, 1–44% and 0.7–2.5% for NAP, PCP and SMX, respectively, as displayed in Figure 4. NAP was the most sorbed compound, in decreasing order by PVC, LDPE and HDPE, with uptake percentages above 25%. The high performance of PVC (67%) may be attributable to several characteristics and related mechanisms: (i) its amorphous structure identified via XRD, facilitating NAP diffusion into the polymeric matrix, (ii) the presence of the highest content of smaller particle fractions from PSD results and (iii) the presence of polar C–Cl bonds and oxidation products detected by FT-IR. PVC characterization suggests the coexistence of a diffusive uptake mechanism associated with amorphous polymer domains and adsorption processes potentially involving surface oxidation products through dipole–dipole interaction.

The concurrence of different uptake mechanisms could also explain the HDPE and LDPE behavior exhibiting a high uptake of NAP (i.e., 26.7 and 32.6%, respectively). Both PEs are among the most crystalline polymers tested in this study, and FT-IR spectra confirmed the aliphatic and non-polar nature of them, suggesting the involvement of hydrophobic interactions in the sorption process.

Similar trends for NAP–MP affinity have been reported in a previous study with sorption capacity decreasing as follows: PVC > LDPE > PP > HDPE [27].

Regarding other polymers, i.e., PET, PP and PS, according to FT-IR results, hydrophobic and π–π interactions appear as the most relevant factors potentially governing the sorption process. The lowest sorption uptake (4%) was observed for PET, in contrast with values exceeding 34% reported by Abbasi et al. [28], which could be attributable to the much higher adsorbent concentration used in their study (50 g/L compared to 1 g/L of the present work). It is worth noting that these authors also highlighted the differences in

PAH sorption reported in the specialized literature explained by variations in MP type and weathering, environmental PAH levels and other environmental factors.

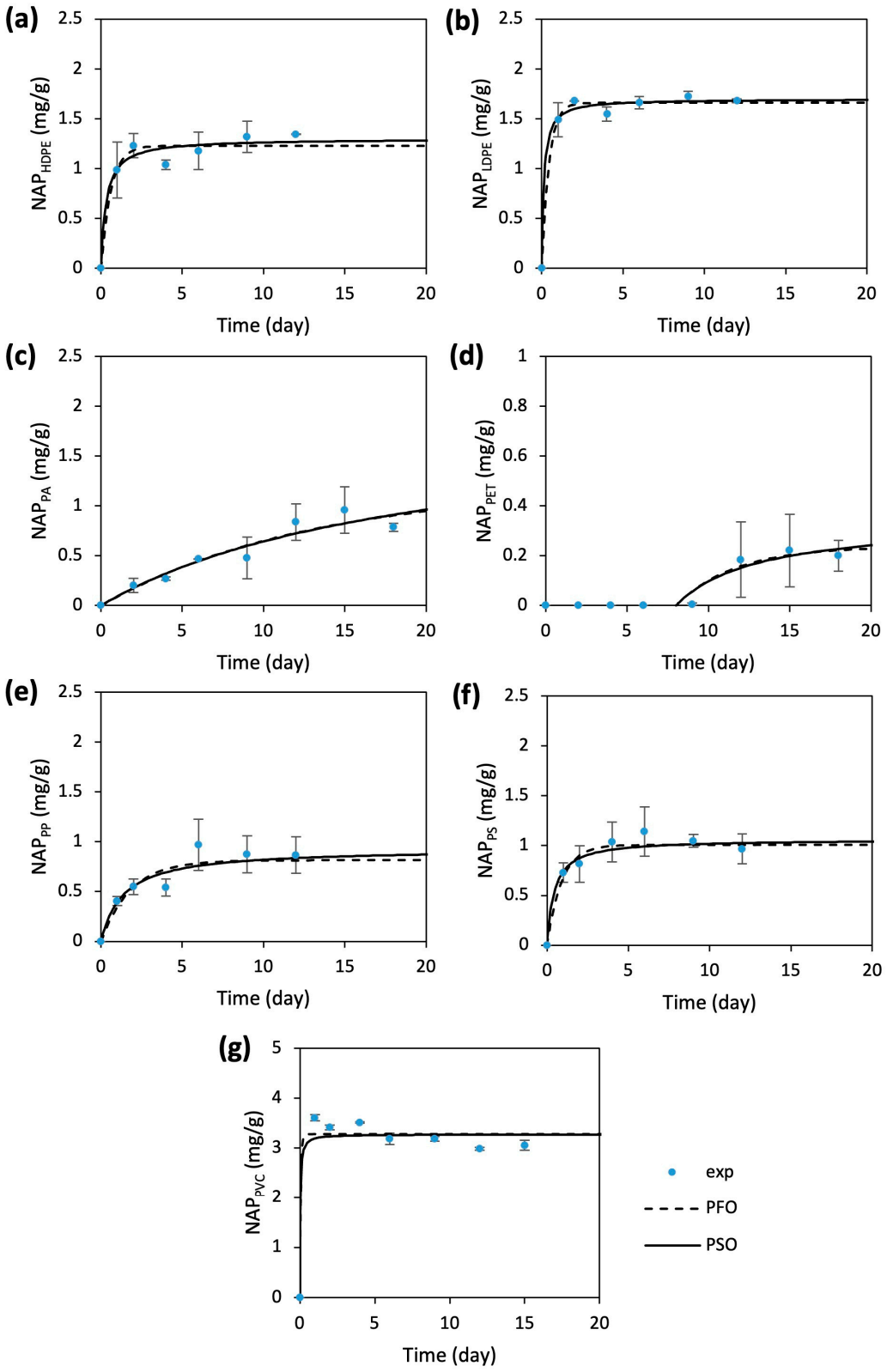

Figure 1. Experimental and predicted time profiles of NAP concentration on tested MPs during sorption tests: HDPE (**a**), LDPE (**b**), PA (**c**), PET (**d**), PP (**e**), PS (**f**), and PVC (**g**).

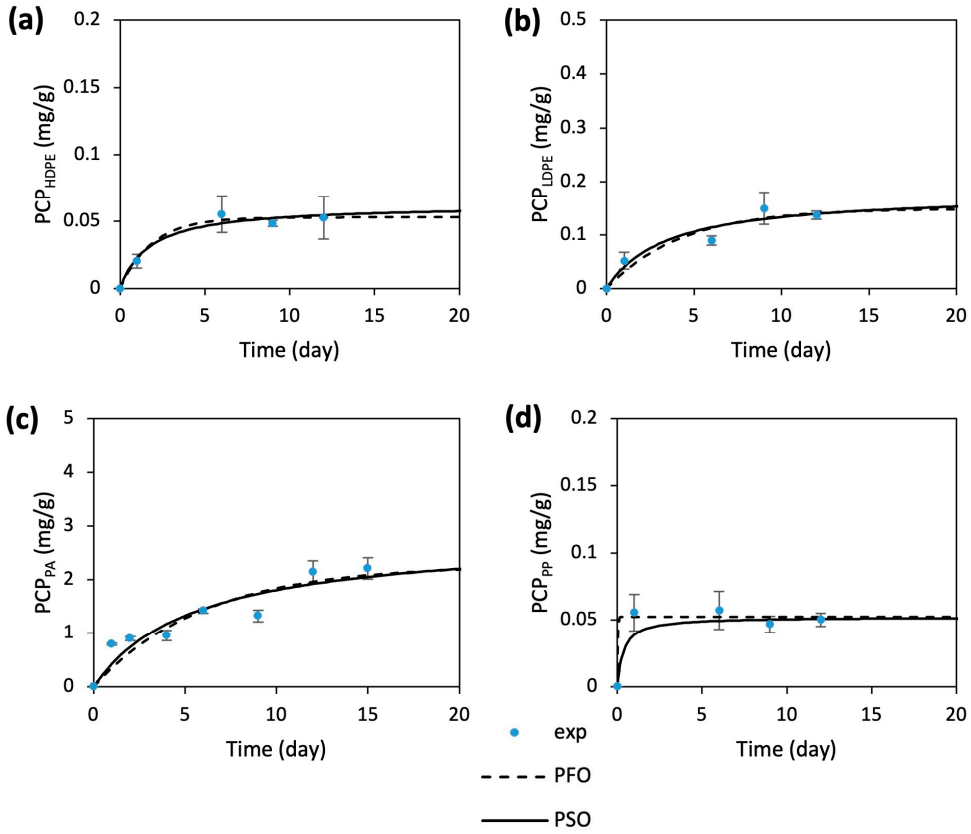

Figure 2. Experimental and predicted time profiles of PCP concentration on tested MPs during sorption tests: HDPE (**a**), LDPE (**b**), PA (**c**), and PP (**d**).

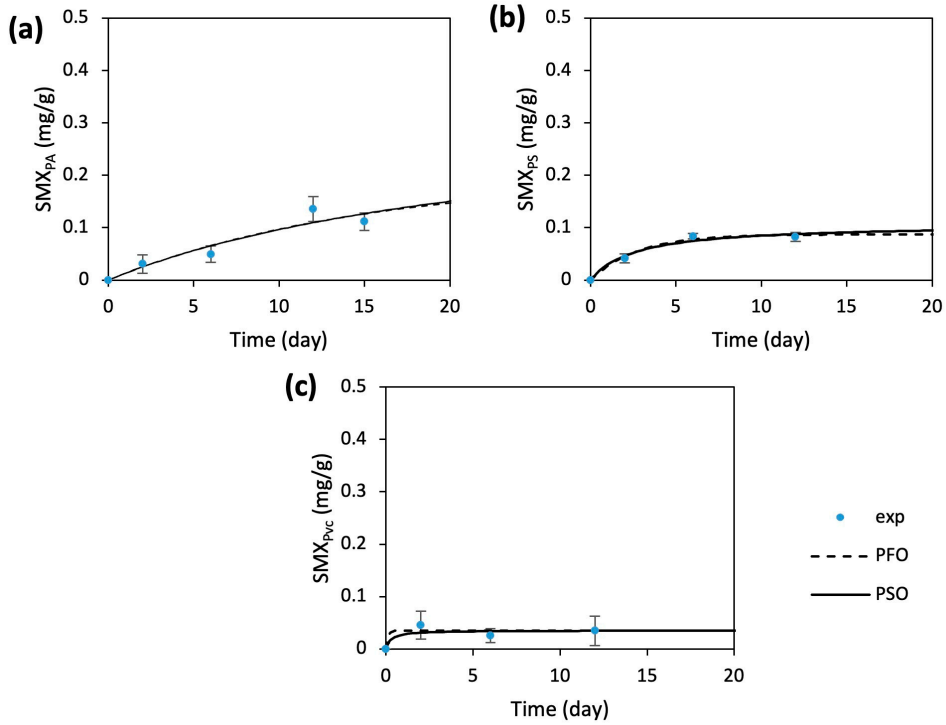

Figure 3. Experimental and predicted time profiles of SMX concentration on tested MPs during sorption tests: PA (**a**), PS (**b**), and PVC (**c**).

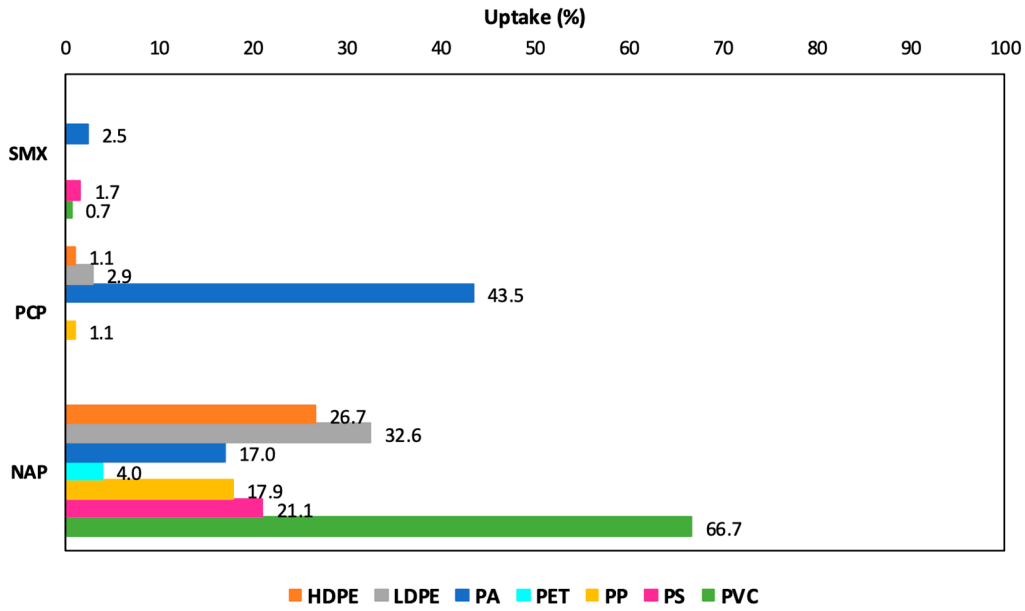

Figure 4. Percentage of uptake of NAP, PCP and SMX onto different MPs (pH 7, $C_{w,0}$ 5 mg/L).

It is worth nothing that PA, as well as being the only MP capable of sorbing three of the four tested compounds, exhibited the greatest sorption capacity for PCP, with an uptake of 43.5% (Figure 4). This value is one order of magnitude greater than the ones detected for the other polymers (from 1.1% for HDPE and PP to 2.9% for LDPE) and the final concentration in MP particles is beyond 2 mg/g (see Figure 2c). This finding could be supported by PSD results, as PA exhibits one of the highest contents of smaller particle fractions, and by FT-IR results revealing amide groups (N–H and C=O) which may facilitate hydrogen bond interactions with the hydroxyl group of PCP. Regarding polyethylene (PE), similarly to PVC-NAP, the presence of minor oxidation products in FT-IR spectra may slightly increase surface polarity, thus increasing their affinity for PCP. Previous works dealing with the sorption of chlorophenols by MPs reported the effective uptake of PCP by PE and PET [32] and by PE and PP [31].

SMX shows low affinity with the investigated polymers (Figure 3a–c) in comparison to other pollutants. Specifically, the sorption of SMX by PA was slightly higher (2.5%) than for other MPs, i.e., PS and PVC (with values within the range of 0.7–1.7%) (Figure 4), probably due the higher polarity of PA and the presence of amino groups that may interact with SMX for the formation of hydrogen bonds [39]. In addition, the low uptake of SMX on PS and PVC can be attributed to the limited interactions arising from aromatic rings (PS) and polar functionalities (PVC). Similarly, Guo et al. [38] investigated SMX sorption by several pristine MPs, including PA, PE, PET, PP, PS and PVC, and observed SMX uptake for PA (>30%) higher than for other MPs (within 5–8%) [39]. Furthermore, previous evidence of SMX uptake by MPs has been reported for PE at 15.3% [36] and around 50% [37], while for PP and PET a value of ~2.5% has been observed [38]. The different orders of magnitude reported for the SMX uptake percentages could be explained by the variability of the operating conditions under which the tests were carried out, as well as by the use of virgin polymeric powder compared to MPs obtained from real plastics.

4.2.2. Kinetic Analysis

Regarding the sorption kinetics, in most cases, the observed sorption pattern includes (i) an initial rapid adsorption (1–2 days) at the fastest rate due to a high availability of unsaturated fraction of polymers and to the highest concentration gradient, (ii) a slow sorption stage (2–6 days), characterized by a progressive decrease in the sorption rate, and

(iii) the final equilibrium stage (6–18 days). Although the duration of each stage varied, this behavior has been observed for the following pairs: NAP-HDPE (Figure 1a), NAP-LDPE (Figure 1b), NAP-PP (Figure 1e), NAP-PS (Figure 1f), NAP-PVC (Figure 1g), PCP-HDPE (Figure 2a), PCP-PP (Figure 2d), and SMX-PVC (Figure 3c). In some cases, the uptake process was particularly fast; for instance, after just one day of contact for some pairs such as NAP-PVC (Figure 1g) and PCP-PP (Figure 2d), the reached polymeric concentrations were comparable to the final levels observed after 12 days. In contrast, other pairs exhibited a different and more gradual uptake process such as PA with all tested pollutants (see Figures 1c, 2c and 3a). In addition, PET with NAP showed an initial lag phase lasting several days before the onset of the sorption process (see Figure 1d).

The t_{eq} values reported in Table 1 represent a qualitative estimation derived from experimental observations, providing an indication of the time required for the uptake process to reach equilibrium. Observed rapid uptakes (t_{eq} of 1–12 days) further highlight the potential role of MPs as vectors of contamination, increasing the likelihood of pollutant transfer when ingested by marine organisms or dispersed through ecosystems.

Table 1. Kinetics data of sorption tests (Bold indicates best fitting model between PFO and PSO).

			PFO				PSO				
MP	**t_{eq}** (d)	**K_1** (1/d)	**$q_{MP,e}$** (mg/g_{MP})	**R^2** -	**CD** -	**SSE** [1] -	**K_2** (g_{MP}/mg d)	**$q_{MP,e}$** (mg/g_{MP})	**R^2** -	**CD** -	**SSE** [1] -
NAP											
HDPE	9	1.674	1.229	0.993	0.953	0.0617	**2.517**	**1.301**	**0.994**	**0.960**	**0.0523**
LDPE	2	**2.316**	**1.660**	**0.999**	**0.992**	**0.0185**	4.695	1.699	0.999	0.992	0.0194
PA	12	**0.078**	**1.200**	**0.978**	**0.921**	**0.1617**	0.027	1.906	0.977	0.919	0.1626
PET [2]	12	**0.275**	**0.237**	**0.966**	**0.914**	**0.0041**	0.574	0.344	0.960	0.898	0.0049
PP	6	**0.549**	**0.814**	**0.970**	**0.860**	**0.0788**	0.779	0.932	0.970	0.856	0.0734
PS	4	**1.128**	**1.006**	**0.989**	**0.931**	**0.0333**	2.172	1.063	0.987	0.921	0.0371
PVC	1	**17.076**	**3.278**	**0.996**	**0.965**	**0.3367**	11.60	3.277	0.995	0.958	0.4127
PCP											
HDPE	6	**0.531**	**0.053**	**0.995**	**0.983**	**$4.09 \cdot 10^{-5}$**	9.064	0.063	0.991	0.969	$7.46 \cdot 10^{-5}$
LDPE	9	0.234	0.149	0.974	0.913	0.0013	**1.615**	**0.179**	**0.978**	**0.925**	**0.0011**
PA	12	0.165	2.273	0.966	0.858	0.5288	**0.062**	**2.831**	**0.971**	**0.878**	**0.4544**
PP	1	**33.75**	**0.052**	**0.994**	**0.969**	**0.0001**	55.00	0.052	0.968	0.843	0.0004
SMX											
PA	12	**0.066**	**0.200**	**0.966**	**0.908**	**0.0004**	0.115	0.341	0.965	0.907	0.0005
PS	6	**0.366**	**0.087**	**0.996**	**0.986**	**$6.47 \cdot 10^{-5}$**	3.563	0.107	0.991	0.972	$1.35 \cdot 10^{-4}$
PVC	2	**8.538**	**0.035**	**0.949**	**0.824**	**$1.98 \cdot 10^{-4}$**	100.0	0.035	0.930	0.756	$2.74 \cdot 10^{-4}$

[1] $SSE = \sum_{i=1}^{n} (q_{cal} - q_{exp})_i^2$, where q_{cal} is the amount of each compound sorbed onto each MP simulated by software at time i, q_{exp} is the experimental amount measured at the same time and *n* are the data points. [2] Starting point for data fitting is t = 8 d.

The PFO (Equation (4)) and PSO (Equation (5)) kinetic models have been applied to correlate kinetic data given their wide employment in modeling the adsorption of solutes from a liquid solution onto solids such as MPs [64]. Figures 1–3 show predicted and experimental concentration profiles vs. time for NAP, PCP and SMX, respectively, while estimated kinetic parameters are reported in Table 1.

A good fitting of the experimental data has been obtained for both models with R^2 values ≥ 0.98 for most cases with a few exceptions. Exceptionally high sorption rates observed for NAP-PVC (Figure 1g), SMX-PVC (Figure 3c) and PCP-PP (Figure 2d) pairs are consistent with rate constants estimated by both models: values listed in Table 1 are at least one order of magnitude greater than for the other tested MP–compound combinations. Comparison of the correlation coefficients obtained for the applied models indicates that, in most cases, R^2 and CD are too close to prevent easy identification of the best-fitting model. Hence, by considering SSE values, the PFO model seems more appropriate to describe

the uptake process of most compound–MP tested pairs, with a few exceptions, including NAP-HDPE and PCP with LDPE and PA, for which R^2 and CD values of the PSO model were also higher than those of the PFO model. These findings may suggest that, in the sorption process for the majority of MP–pollutant pairs, physical rather than chemical bonds should prevail since the sorption process described by the PFO model does not involve significant chemical sorption or complex interactions that are typically explained by the PSO model. However, given the minimal differences in correlation coefficients between the two kinetic models, it remains difficult to identify the optimal model that uniquely describes experimental data. A possible explanation of these results is the concomitance of different sorption mechanisms during the uptake process.

Analysis of literature data for the different target pollutants highlighted wide intervals for kinetic parameters: for instance, for NAP a value of K_2 of 1.61 mg/g d has been reported for PS [26], which is consistent with the values estimated in this study. Different values are reported for other MPs, from 0.008–0.016 g/mg d for HDPE [29] up to values of 7.2, 86.4 and 280 g/mg d for PE, PP and PET, respectively [30]. Reported K_2 values for PCP are within the range of 0.05–0.21 (g/mg d) for PP and PE, respectively [31], while for SMX reported K_2 values are higher, e.g., 240 g/mg d for PA [65] and 190–240 g/mg d [36,37] for PE. These marked differences may be due to different reasons: the empirical nature of the models, the unavoidable variations in the operating conditions applied in the sorption tests and, more importantly, the different behavior of pristine, commercial and real MPs.

4.2.3. Partition Coefficient Evaluation

The partitioning of chemicals between two phases is a dynamic process and a state of equilibrium is reached when the concentrations in both phases become constant. Equilibrium data of contaminant concentrations in MPs (Figure 5) and aqueous phases (Figure S7) have been employed to calculate PCs according to Equation (3): Table 2 displays PC values for each MP–pollutant combination tested and the "experimental" order of affinity, estimated according to the PC ranking.

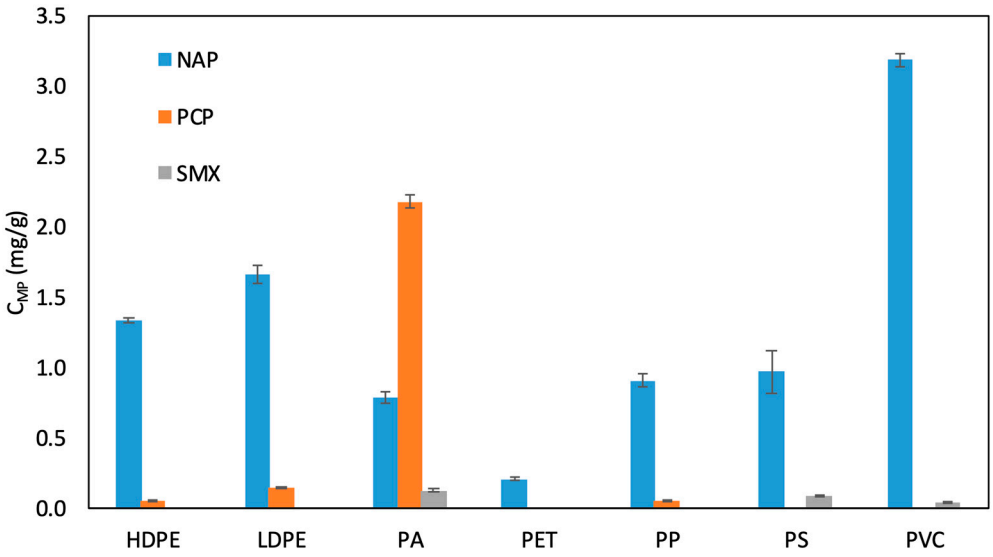

Figure 5. Polymeric concentrations of target compounds at equilibrium conditions for different MPs (pH 7, $C_{w,0}$ 5 mg/L). Data are reported as average values (±SD) calculated for the different samples taken after equilibrium was reached until the end of the tests.

Table 2. PCs (L/kg) with standard deviation (SD) in parentheses for target pollutants associated with the tested MPs and experimental order of affinity from tests at pH 7 (*ns*: no sorption observed). Italics in "Experimental Order of Affinity" column indicates no sorption observed.

	NAP	PCP	SMX	IBU	Experimental Order of Affinity
HDPE	372.8 (0.5)	10.8 (0.7)	*ns*	*ns*	NAP > PCP >> *SMX = IBU*
LDPE	515.4 (37.2)	29.9 (1.9)	*ns*	*ns*	NAP > PCP >> *SMX = IBU*
PA	204.0 (19.6)	717.8 (44.4)	25.5 (2.6)	*ns*	PCP > NAP > SMX >> *IBU*
PET	41.4 (3.9)	*ns*	*ns*	*ns*	NAP >> *PCP = SMX = IBU*
PP	213.1 (15.7)	10.7 (1.0)	*ns*	*ns*	NAP > PCP >> *SMX = IBU*
PS	252.7 (23.8)	*ns*	17.0 (0.1)	*ns*	NAP > SMX >> *PCP = IBU*
PVC	1934.2 (331.2)	*ns*	7.1 (1.1)	*ns*	NAP > SMX >> *PCP = IBU*

As expected, PC values of most polymers for NAP are higher than for other pollutants, with the only exception being PCP for PA. Moreover, partition data are quite consistent with previous studies. The range of values of PC reported for NAP is very broad, from 300 (L/kg) for PVC [66] to 865 L/kg for PE [67] and up to 11,965·10^3 L/kg reported for PS [26]. Reported data dealing with the partition of PCP onto MPs range from 10–50 L/kg for PET and HDPE [33] and up to values over 500·10^3 L/kg for PET [32]. These values, in particular the ones obtained from real MPs, are quite consistent with data obtained in this study, especially for PP (10.7 L/kg), HDPE (10.8 L/kg) and LDPE (29.9 L/kg). Literature data for SMX are within the range of 20 L/kg for PET and 284 L/kg for PA, as reported by Guo et al. [39] who, as mentioned above, among different polymers, including PA, PE, PET, PP, PS and PVC, noticed PA as the polymer with the highest affinity for antibiotics. On the contrary, lower values are reported for PA and PS (8–26 and 7–21 L/kg, respectively) [68] and for PE (30 L/kg), PP (30.9 L/kg), PS (29.7 L/kg) and PVC (28.2 L/kg) [69]. Similar values have been obtained in this study, with values from 7.1 L/kg for PVC to 25.5 L/kg for PA. In any case, as already pointed out, a direct comparison of literature data is not so significant because PC values are dependent on many experimental factors such as particle size, morphology, and surface modifications and on the properties of the background solution [70].

PC values have also been evaluated with equilibrium polymeric concentrations predicted by the application of both PFO and PSO kinetic models (reported in Table 1) by using Equation (3) and aqueous concentrations reported in Figure S7. Figure 6 displays the comparison of PC values obtained from experimental and predicted data, whose difference is not statistically significant ($p > 0.05$) for both tested models.

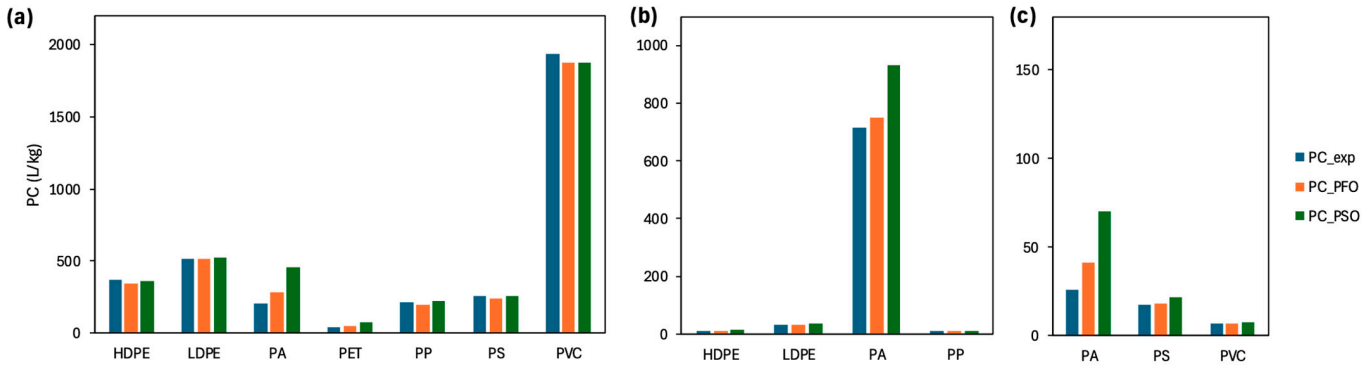

Figure 6. Comparison of PC values for NAP (**a**), PCP (**b**) and SMX (**c**) obtained from experimental (PC_exp) and predicted data from PFO (PC_PFO) and PSO (PC_PSO) models.

4.2.4. Effect of pH on the Sorption Process of Ionizable Compounds—The Case Study of SMX

Sorption of ionizable compounds is affected by their ionization state in the tested operating conditions, and, among the compounds investigated in this study, the behavior of PCP, IBU and SMX can be influenced by this factor.

PCP is characterized by a pKa of 4.7–4.8, thus in acidic conditions (that is pH < pKa) neutral species dominate, favoring hydrophobic interactions with MPs, while at higher pH, negatively charged PCP ions (i.e., pentachlorophenate) are repelled. Higher PCP sorption is expected for amorphous polymers at low pH due to the diffusion process of the undissociated species, while at pH close to neutrality (or higher) the sorption process (via diffusion) of anionic species is disadvantaged. This could explain the no sorption observed in this study at neutral pH for PS and PVC, which are predominantly amorphous, and partially explain the negligible sorption onto the semicrystalline PET.

Similar conditions occur for IBU characterized by pKa of 4.4–4.6, and in this case in acidic conditions the compound exists predominantly in its protonated, neutral (unionized) form, while for pH above the pKa, the carboxylic acid group deprotonates, generating the anionic (carboxylate) form. The compound is completely dissociated at pH $\geq$ 7.5. Although also in this case the speciation at different pH could influence the sorption on MPs, the practically negligible uptake observed for all investigated MPs suggests a combined effect of different factors and interactions in determining this condition.

More complex is the speciation of SMX at different pH: sulfonamide antibiotics such SMX contain a basic amino group (–NH_2) and an acidic amino group (–NH–); therefore, they haves two dissociation constants, i.e., pKa_1 of 1.7 and pKa_2 of 5.7 [71], making the identification of factors affecting the sorption mechanism on MPs more difficult. To deeply investigate this aspect, additional sorption tests for SMX have been conducted at pH 4. Results are shown in Figures 7 and S8: it is observed that decreasing pH from neutrality to 4 exerts a double effect on the sorption of SMX in terms of sorption capacity and kinetics. Data comparison at pH 7 and 4 shows that all tested MPs sorb SMX in acidic conditions, while at neutral conditions SMX uptake is observed only for PA, PS and PVC (Figure 7a). Moreover, greater concentrations in polymers have been detected, especially for PS and PVC (Figure 7c) and equilibrium conditions were achieved faster than in neutral conditions (Figure 7b). Equilibrium data have been utilized to calculate PCs at pH 4, with the same method applied for pH 7. Figure 7d highlights the relevant impact of decreasing pH on sorption capacity in equilibrium conditions, resulting in PC values much higher than those observed at pH 7.

Several studies supported the positive effect of low pH on the sorption process of SMX by MPs [38,39,65]. This can be attributable to the different mechanisms occurring, depending on the pH and related speciation. At a pH below 1.7, the predominant ion species is positively charged, which can be adsorbed on negatively charged polymeric surfaces; at pH in the range of 1.7 and 5.7, the dominant species is the neutral one, which is subject to diffusion into the polymeric matrix. When the pH exceeds 5.7, the negatively charged SMX^- becomes the primary ion species, increasing electrostatic repulsion and reducing SMX sorption by negatively charged MPs. This suggests that electrostatic interactions exert a key role in the mechanism governing the sorption process at neutral pH.

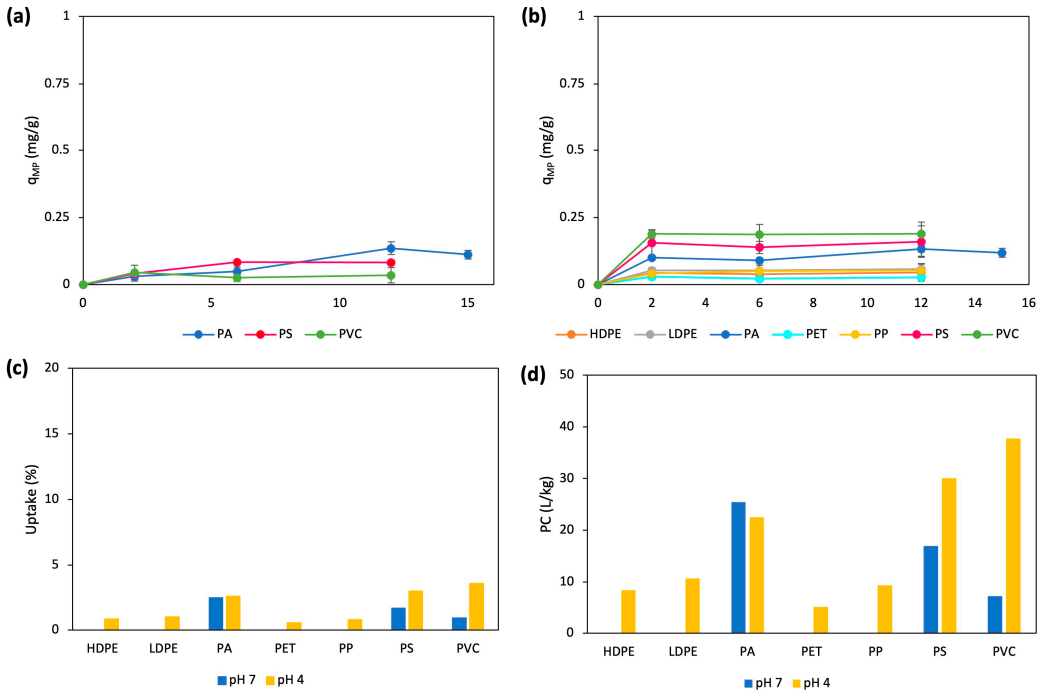

Figure 7. Experimental time profile of polymeric concentrations of SMX at pH 7 (**a**) and pH 4 (**b**), uptake percentage observed at pH 4 and pH 7 (**c**) and PC values estimated for both conditions from equilibrium data (**d**).

4.3. Theoretical Thermodynamic Predictions of Sorption Scenarios by HSP

To predict the uptake and subsequent diffusion of pollutants onto MPs, an HSP framework was utilized to estimate thermodynamic affinity between plastic debris and contaminants through the determination of the relative Ra distances for each MP–pollutant pair (Table 3). As mentioned above, a low Ra distance indicates high molecular affinity of the contaminant for the plastic, leading to a significant sorption potential. Conversely, a large Ra distance suggests weak interactions and limited uptake by plastics.

Table 3. Ra distances ($MPa^{1/2}$) for target pollutants associated with the tested MPs and predicted order of affinity. Italics in "Predicted Order of Affinity" column indicates no significant sorption observed in experimental tests and bold indicates discrepancies between experimental and predicted order of affinity.

	NAP	PCP	SMX	IBU	Predicted Order of Affinity	Experimental Validation
HDPE	5.0	14.6	19.7	32.7	NAP > PCP > *SMX* > *IBU*	✓
LDPE	6.9	13.3	15.2	28.0	NAP > PCP > *SMX* > *IBU*	✓
PA	8.6	6.9	11.8	20.2	PCP > NAP > SMX > *IBU*	✓
PET	6.0	8.2	10.7	23.9	NAP > *PCP* > *SMX* > *IBU*	✓
PP	6.7	16.1	20.8	34.4	NAP > PCP > *SMX* > *IBU*	✓
PS	4.7	10.9	13.9	28.6	NAP > ***PCP*** > **SMX** > *IBU*	partial
PVC	6.9	9.3	10.4	25.3	NAP > ***PCP*** > **SMX** > *IBU*	partial

Based on Ra distances reported in Table 3, the resulting "predicted" order of affinity has been evaluated. The first evidence is that NAP, i.e., the most apolar compound, shows the highest thermodynamic affinity with all the polymers, with the only exception being PA (nylon 6,6 in this study), the only one with an amino group. The highest affinity for PA is detected for PCP (Ra distance of 6.9 and 8.6 $MPa^{½}$ for PCP and NAP, respectively). Low affinity for most MPs under investigation is observed for SMX, showing high values of Ra

distances (within the range of 10.4–20.8 $MPa^{½}$). This outcome could be explained by the highest content of polar groups in SMX, including a sulfonamide group ($-SO_2NH_2$) and a heterocyclic group with nitrogen. Finally, IBU shows the lowest affinity for all polymers, indeed, values of Ra distances estimated for this compound are effectively higher than for other pollutants, suggesting very low sorption capacities by those polymers, as confirmed by experimental sorption tests.

The consistence of the single partial parameters δ and the difference among them provide insights into the type of intermolecular forces dominating the sorption process, based on compound properties. For example, PCP is characterized by high δ_H and relatively low δ_P that likely relies on hydrogen bonding as a key sorption mechanism, while SMX with high δ_P and moderate δ_H might exhibit dipolar interaction dominance. Likewise, NAP is the pollutant with the highest dispersion parameter value, in addition to very low polar and hydrogen-bonding parameters; this condition reflects non-polar interactions such as van der Waals forces.

4.4. Validation of Theoretical Predictive Approach and Implications of Its Use

Experimental data obtained from sorption tests have been used in this study to give a first validation of HSP predictions based on thermodynamic affinity between tested MPs and pollutants. In general, the predictive sorption scenarios evaluated by HSP data are consistent with experimental observations. Indeed, Table 2 reports the order of affinity evaluated from experimental data: the direct comparison of these rankings with those obtained from HSP method (see Table 3) indicates that almost the totality of the predictions aligns with experimental results and PC estimations. The observed differences between experimental and predicted order of affinity are highlighted in Table 3 by bold text and are limited to PS and PVC for only two pollutants, i.e., SMX and PCP. In addition, it is worth noting that SMX and IBU exhibit similar behavior for HDPE, LDPE, PP and PET whereas IBU and PCP for PET, PS and PVC. In these cases, no detectable sorption by these polymers was observed (highlighted in italics in Table 2), hence there is no meaningful difference for experimental order of affinity for these compounds by the mentioned polymers.

The discrepancies observed between experimental and predicted affinity rankings in systems involving polymers may be due to several reasons. Firstly, testing commercial polymers obtained from real items, although effective in reproducing realistic conditions, can be a limitation for HSP method application. This is because real plastics are not fully described by HSP coefficients, which are usually available for pure polymers [10] or can be theoretically estimated only if the complete chemical composition is known. Indeed, the presence of additives, colorants and other compounds in real MPs are not included in HSP values and thus in the predictive sorption scenarios. Support for this hypothesis is given by XRD spectra (Figure S3f,g) revealing the presence of $CaCO_3$ fillers in PS and PVC components, which may significantly influence the actual sorption capacity of these polymers. Additionally, the HSP framework does not explicitly account for physical factors such as particle size, pore size, crystallinity, chain mobility, aging and weathering or environmental factors (temperature, pH and so on), all of which can influence sorption as also observed in this study. For example, the oxidation products detected by FT-IR on the surface of "real" MPs (like PVC and, to a minor extent, HDPE and LDPE) introduce polarities that differ from the pristine chemical structures assumed in HSP-based thermodynamic modeling.

Furthermore, sorption is a complex process governed by multiple mechanisms, including hydrophobic interactions, partition, electrostatic interactions, and other non-covalent interactions. The relative contribution of each mechanism is strongly influenced by many properties of both the sorbent (fractions of crystallinity and amorphous regions, hardness,

polarity, etc.) and the compound (hydrophobicity, ionic properties), as well as environmental factors, which are not explicitly accounted for in the prediction.

Despite the limitations discussed above, the results of this study indicate that the HSP-based approach provides a valid theoretical methodology for a first evaluation of thermodynamic affinities, enabling qualitative predictions of the potential uptake of contaminants by MPs acting as contaminant vectors. In particular, HSP-derived predictions can be employed to define and to optimize experimental strategies as well as to integrate the information required by robust modeling of the uptake process at a microscale level (in the MP particles) and the contaminant diffusion at a macroscale level in the different environmental compartments.

5. Conclusions

This study provides a comprehensive evaluation of the sorption behaviors of multiple pollutants onto various MP polymers, integrating both experimental and theoretical approaches. The results demonstrate that the contaminant uptake is strongly dependent on interactions determined by the properties of the pollutant and the polymer type. Among the tested compounds, NAP showed the highest sorption across the majority of tested polymers, PCP exhibited selective but substantial uptake, and SMX displayed low affinity, except for specific polymers under acidic conditions (pH 4). Kinetic analyses reveal predominantly rapid initial sorption followed by a slower approach to equilibrium, underscoring the MPs' potential to quickly accumulate environmental contaminants. Equilibrium and partition data further highlighted the complexity of the sorption process, governed by many factors such as hydrophobicity, specific molecular interactions, chemical and physical characteristics of the MPs and additional specific factors, such as pH and particle size. Validation of the HSP-based thermodynamic predictions with experimental data suggests that this method can provide a first estimation of the relative affinities of organic pollutants for different MPs even if limitations inherent to real-world MP heterogeneity and environmental conditions need further investigations. Overall, the integration of empirical results with thermodynamic modeling underscores the utility of the HSP approach as a valuable screening tool for anticipating contaminant–MP interactions and for designing targeted experimental and environmental risk assessment tools.

Supplementary Materials: The following supporting information can be downloaded at: https://www.mdpi.com/article/10.3390/microplastics5020082/s1, Section S1: MP characterization; Section S2: Validation of analytical methods; Section S3. Sorption tests: control tests; Figure S1: Commercial plastic stuff used to produce tested microplastic particles (a) and some pictures of plastic processing during their preparation (b–d); Figure S2: Cumulative and discrete mass distribution of MP samples: data of HDPE (a,b), LDPE (c,d), PA (e,f), PET (g,h), PP (i,j), PS (k,l), and PVC (m,n); Figure S3: XRD spectra of MP samples of HDPE (a), LDPE (b), PA (c), PET (d), PP (e), PS (f), and PVC (g); Figure S4: FT-IR spectra of MP samples of HDPE (a), LDPE (b), PA (c), PET (d), PP (e), PS (f), and PVC (g); Figure S5: Experimental time profiles of aqueous concentration of NAP (a), PCP (b), IBU (c) and SMX (d) during sorption tests; Figure S6: Experimental time profiles of aqueous concentration in control tests (without MPs) of NAP (a), PCP (b), IBU (c) and SMX (d) during sorption tests. Data are reported as average values (bars are SD) calculated for the different control samples collected at the same times; Figure S7: Aqueous concentrations of target compounds for different MPs (pH 7, $C_{w,0}$ 5 mg/L) in equilibrium conditions for PC calculation. Data are reported as average values calculated for the different samples once equilibrium was reached and bars are SD among all equilibrium samples; Figure S8: Results of sorption tests of SMX performed at pH 4 ($C_{w,0}$ 5 mg/L): experimental time profiles of aqueous concentration of SMX for different MPs during sorption tests (a) and aqueous concentrations at equilibrium conditions for PC calculation ((b), data are reported as average values calculated for the different samples once equilibrium was reached and bars are

SD among all equilibrium samples); Table S1: Sorption studies of different MPs in combination with NAP, PCP, IBU and SMX; Table S2: Operating conditions for SMX and IBU analytical determinations; Table S3: HSPs for MPs and pollutants tested in this study; Table S4: Granulometric data from PSD characterization.

Author Contributions: Conceptualization, D.M.A. and M.C.T.; methodology, D.M.A. and E.D.; software, D.M.A.; validation, D.M.A., E.D. and M.C.T.; formal analysis, D.M.A. and E.D.; investigation, D.M.A. and M.M.; resources, M.C.T.; data curation, D.M.A.; writing—original draft preparation, D.M.A. and E.D.; writing—review and editing, E.D., M.M. and M.C.T.; visualization, D.M.A.; supervision, M.C.T.; project administration, M.C.T. All authors have read and agreed to the published version of the manuscript.

Funding: This research received no external funding.

Institutional Review Board Statement: Not applicable.

Data Availability Statement: The original contributions presented in the study are included in the article and Supplementary Material, further inquiries can be directed to the corresponding author.

Acknowledgments: We would like to thank Laura Lilla of the Institute for Biological Systems, National Research Council (CNR-ISB) for her valuable contribution in chemical analysis during this study and Daniele Passeri of the Institute of Environmental Geology and Geoengineering, National Research Council (CNR-IGAG) for his helpful contribution in granulometric analysis for this study. We gratefully acknowledge the SURFACE facility of the Institute of Nanostructured Materials, National Research Council (CNR-ISMN) for performing the XRD and FT-IR measurements and for the valuable collaboration and for the technical support provided during the experimental work.

Conflicts of Interest: The authors declare no conflicts of interest.

Abbreviations

The following abbreviations are used in this manuscript:

ACN	Acetonitrile
ATR	Attenuated total reflectance
CD	Coefficient of determination
FT-IR	Fourier transform infrared
HDPE	High-density polyethylene
HSP	Hansen solubility parameter
IBU	Ibuprofen
LDPE	Low-density polyethylene
LOD	Limit of detection
LOQ	Limit of quantification
MP	Microplastic
NAP	Naphthalene
PA	Polyamide
PAHs	Polycyclic aromatic hydrocarbons
PC	Partition coefficient
PCP	Pentachlorophenol
PLA	Polylactic acid
PE	Polyethylene
PET	Polyethylene terephthalate
PFO	Pseudo-first order
PP	Polypropylene
PS	Polystyrene
PSD	Particle size distribution
PSO	Pseudo-second order

PVC	Polyvinyl chloride
RSD	Relative standard deviation
SD	Standard deviation
SMX	Sulfamethoxazole
SSE	Sum of squared errors
XRD	X-ray diffraction

References

1. Yousafzai, S.; Farid, M.; Zubair, M.; Naeem, N.; Zafar, W.; Zaman Asam, Z.U.; Farid, S.; Ali, S. Detection and Degradation of Microplastics in the Environment: A Review. *Environ. Sci. Adv.* **2025**, *4*, 1142–1165. [CrossRef]
2. He, B.; Smith, M.; Egodawatta, P.; Ayoko, G.A.; Rintoul, L.; Goonetilleke, A. Dispersal and Transport of Microplastics in River Sediments. *Environ. Pollut.* **2021**, *279*, 116884. [CrossRef]
3. Xu, S.; Ma, J.; Ji, R.; Pan, K.; Miao, A.-J. Microplastics in Aquatic Environments: Occurrence, Accumulation, and Biological Effects. *Sci. Total Environ.* **2020**, *703*, 134699. [CrossRef]
4. Banaee, M.; Multisanti, C.R.; Impellitteri, F.; Piccione, G.; Faggio, C. Environmental Toxicology of Microplastic Particles on Fish: A Review. *Comp. Biochem. Physiol. Part C Toxicol. Pharmacol.* **2025**, *287*, 110042. [CrossRef]
5. Sun, N.; Shi, H.; Li, X.; Gao, C.; Liu, R. Combined Toxicity of Micro/Nanoplastics Loaded with Environmental Pollutants to Organisms and Cells: Role, Effects, and Mechanism. *Environ. Int.* **2023**, *171*, 107711. [CrossRef]
6. Costigan, E.; Collins, A.; Hatinoglu, M.D.; Bhagat, K.; MacRae, J.; Perreault, F.; Apul, O. Adsorption of Organic Pollutants by Microplastics: Overview of a Dissonant Literature. *J. Hazard. Mater. Adv.* **2022**, *6*, 100091. [CrossRef]
7. Agboola, O.D.; Benson, N.U. Physisorption and Chemisorption Mechanisms Influencing Micro (Nano) Plastics-Organic Chemical Contaminants Interactions: A Review. *Front. Environ. Sci.* **2021**, *9*, 678574. [CrossRef]
8. Fu, L.; Li, J.; Wang, G.; Luan, Y.; Dai, W. Adsorption Behavior of Organic Pollutants on Microplastics. *Ecotoxicol. Environ. Saf.* **2021**, *217*, 112207. [CrossRef]
9. Town, R.M.; van Leeuwen, H.P.; Duval, J.F.L. Sorption Kinetics of Metallic and Organic Contaminants on Micro- and Nanoplastics: Remarkable Dependence of the Intraparticulate Contaminant Diffusion Coefficient on the Particle Size and Potential Role of Polymer Crystallinity. *Environ. Sci. Process. Impacts* **2025**, *27*, 634–648. [CrossRef] [PubMed]
10. Hansen, C.M. *Hansen Solubility Parameters: A User's Handbook*, 2nd ed.; CRC Press: Boca Raton, FL, USA, 2007.
11. Khansary, M.A.; Mellat, M.; Saadat, S.H.; Fasihi-Ramandi, M.; Kamali, M.; Taheri, R.A. An Enquiry on Appropriate Selection of Polymers for Preparation of Polymeric Nanosorbents and Nanofiltration/Ultrafiltration Membranes for Hormone Micropollutants Removal from Water Effluents. *Chemosphere* **2017**, *168*, 91–99. [CrossRef]
12. Poleo, E.E.; Daugulis, A.J. A Comparison of Three First Principles Methods for Predicting Solute–Polymer Affinity, and the Simultaneous Biodegradation of Phenol and Butyl Acetate in a Two-Phase Partitioning Bioreactor. *J. Chem. Technol. Biotechnol.* **2014**, *89*, 88–96. [CrossRef]
13. Tomei, M.C.; Mosca Angelucci, D.; Stazi, V.; Daugulis, A.J. On the Applicability of a Hybrid Bioreactor Operated with Polymeric Tubing for the Biological Treatment of Saline Wastewater. *Sci. Total Environ.* **2017**, *599–600*, 1056–1063. [CrossRef]
14. Mosca Angelucci, D.; Tomei, M.C. Uptake/Release of Organic Contaminants by Microplastics: A Critical Review of Influencing Factors, Mechanistic Modeling, and Thermodynamic Prediction Methods. *Crit. Rev. Environ. Sci. Technol.* **2022**, *52*, 1356–1400. [CrossRef]
15. Lionetto, F.; Esposito Corcione, C.; Messa, F.; Perrone, S.; Salomone, A.; Maffezzoli, A. The Sorption of Amoxicillin on Engineered Polyethylene Terephthalate Microplastics. *J. Polym. Environ.* **2023**, *31*, 1383–1397. [CrossRef]
16. Mosca Angelucci, D.; Piergiacomo, F.; Donati, E.; Pagani, L.; Minuti, E.; Brusetti, L.; Tomei, M.C. Combined Effects of Ciprofloxacin and Microplastics on Alpine Spring Water Microbiota: Evidence from Glacier-Fed Microcosm Experiments. *Front. Microbiol.* **2025**, *16*, 1654589. [CrossRef] [PubMed]
17. Paul-Pont, I.; Tallec, K.; Gonzalez-Fernandez, C.; Lambert, C.; Vincent, D.; Mazurais, D.; Zambonino-Infante, J.L.; Brotons, G.; Lagarde, F.; Fabioux, C.; et al. Constraints and Priorities for Conducting Experimental Exposures of Marine Organisms to Microplastics. *Front. Mar. Sci.* **2018**, *5*, 252. [CrossRef]
18. Duis, K.; Coors, A. Microplastics in the Aquatic and Terrestrial Environment: Sources (with a Specific Focus on Personal Care Products), Fate and Effects. *Environ. Sci. Eur.* **2016**, *28*, 2. [CrossRef]
19. Plastic Europe Plastics—The Fast Facts 2024. Available online: https://plasticseurope.org/knowledge-hub/plastics-the-fast-facts-2024/ (accessed on 1 April 2026).
20. Ravit, B.; Cooper, K.; Buckley, B.; Yang, I.; Deshpande, A. Organic Compounds Associated with Microplastic Pollutants in New Jersey, U.S.A. Surface Waters. *AIMS Environ. Sci.* **2019**, *6*, 445–459. [CrossRef]

21. Wang, F.; Wong, C.S.; Chen, D.; Lu, X.; Wang, F.; Zeng, E.Y. Interaction of Toxic Chemicals with Microplastics: A Critical Review. *Water Res.* **2018**, *139*, 208–219. [CrossRef]
22. Lee, H.; Shim, W.J.; Kwon, J.-H. Sorption Capacity of Plastic Debris for Hydrophobic Organic Chemicals. *Sci. Total Environ.* **2014**, *470–471*, 1545–1552. [CrossRef]
23. Wu, C.-C.; Bao, L.-J.; Liu, L.-Y.; Shi, L.; Tao, S.; Zeng, E.Y. Impact of Polymer Colonization on the Fate of Organic Contaminants in Sediment. *Environ. Sci. Technol.* **2017**, *51*, 10555–10561. [CrossRef]
24. Altomare, A.; Corriero, N.; Cuocci, C.; Falcicchio, A.; Moliterni, A.; Rizzi, R. QUALX2.0: A Qualitative Phase Analysis Software Using the Freely Available Database POW_COD. *J. Appl. Crystallogr.* **2015**, *48*, 598–603. [CrossRef]
25. Wang, W.; Wang, J. Different Partition of Polycyclic Aromatic Hydrocarbon on Environmental Particulates in Freshwater: Microplastics in Comparison to Natural Sediment. *Ecotoxicol. Environ. Saf.* **2018**, *147*, 648–655. [CrossRef] [PubMed]
26. Yu, H.; Yang, B.; Waigi, M.G.; Peng, F.; Li, Z.; Hu, X. The Effects of Functional Groups on the Sorption of Naphthalene on Microplastics. *Chemosphere* **2020**, *261*, 127592. [CrossRef] [PubMed]
27. Wang, J.; Liu, X.; Liu, G. Sorption Behaviors of Phenanthrene, Nitrobenzene, and Naphthalene on Mesoplastics and Microplastics. *Environ. Sci. Pollut. Res.* **2019**, *26*, 12563–12573. [CrossRef] [PubMed]
28. Abbasi, S.; Moore, F.; Keshavarzi, B. PET-Microplastics as a Vector for Polycyclic Aromatic Hydrocarbons in a Simulated Plant Rhizosphere Zone. *Environ. Technol. Innov.* **2021**, *21*, 101370. [CrossRef]
29. Funari, R.A.; Frescura, L.M.; de Menezes, B.B.; Bastos, A.F.d.M.; da Rosa, M.B. Adsorption of Naphthalene and Its Derivatives onto High-Density Polyethylene Microplastic: Computational, Isotherm, Thermodynamic, and Kinetic Study. *Environ. Pollut.* **2023**, *318*, 120919. [CrossRef]
30. Lončarski, M.; Gvoić, V.; Prica, M.; Cveticanin, L.; Agbaba, J.; Tubić, A. Sorption Behavior of Polycyclic Aromatic Hydrocarbons on Biodegradable Polylactic Acid and Various Nondegradable Microplastics: Model Fitting and Mechanism Analysis. *Sci. Total Environ.* **2021**, *785*, 147289. [CrossRef]
31. Tubić, A.; Lončarski, M.; Maletić, S.; Jazić, J.M.; Watson, M.; Tričković, J.; Agbaba, J. Significance of Chlorinated Phenols Adsorption on Plastics and Bioplastics during Water Treatment. *Water* **2019**, *11*, 2358. [CrossRef]
32. Lončarski, M.; Tubic, A.; Isakovski, M.K.; Jovic, B.; Apostolovic, T.; Nikic, J.; Agbaba, J. Modelling of the Adsorption of Chlorinated Phenols on Polyethylene and Polyethylene Terephthalate Microplastic. *J. Serbian Chem. Soc.* **2020**, *85*, 697–709. [CrossRef]
33. Miranda, M.N.; Lado Ribeiro, A.R.; Silva, A.M.T.; Pereira, M.F.R. Can Aged Microplastics Be Transport Vectors for Organic Micropollutants?—Sorption and Phytotoxicity Tests. *Sci. Total Environ.* **2022**, *850*, 158073. [CrossRef]
34. Martín, C.; Fajardo, C.; Costa, G.; Sánchez-Fortún, S.; San Andrés, M.D.; González, F.; Nande, M.; Mengs, G.; Martín, M. Bioassays to Assess the Ecotoxicological Impact of Polyethylene Microplastics and Two Organic Pollutants, Simazine and Ibuprofen. *Chemosphere* **2021**, *274*, 129704. [CrossRef] [PubMed]
35. Fajardo, C.; Sánchez-Fortún, S.; Videira-Quintela, D.; Martin, C.; Nande, M.; D'ors, A.; Costa, G.; Guillen, F.; Montalvo, G.; Martin, M. Biofilm Formation on Polyethylene Microplastics and Their Role as Transfer Vector of Emerging Organic Pollutants. *Environ. Sci. Pollut. Res.* **2023**, *30*, 84462–84473. [CrossRef] [PubMed]
36. Razanajatovo, R.M.; Ding, J.; Zhang, S.; Jiang, H.; Zou, H. Sorption and Desorption of Selected Pharmaceuticals by Polyethylene Microplastics. *Mar. Pollut. Bull.* **2018**, *136*, 516–523. [CrossRef] [PubMed]
37. Xu, B.; Liu, F.; Brookes, P.C.; Xu, J. The Sorption Kinetics and Isotherms of Sulfamethoxazole with Polyethylene Microplastics. *Mar. Pollut. Bull.* **2018**, *131*, 191–196. [CrossRef]
38. Kong, F.; Xu, X.; Xue, Y.; Gao, Y.; Zhang, L.; Wang, L.; Jiang, S.; Zhang, Q. Investigation of the Adsorption of Sulfamethoxazole by Degradable Microplastics Artificially Aged by Chemical Oxidation. *Arch. Environ. Contam. Toxicol.* **2021**, *81*, 155–165. [CrossRef]
39. Guo, X.; Chen, C.; Wang, J. Sorption of Sulfamethoxazole onto Six Types of Microplastics. *Chemosphere* **2019**, *228*, 300–308. [CrossRef]
40. Werle-Wilczyńska, A.; Ciecierska-Stokłosa, D.; Gorczyńska, K.; Gluzińska, M. Ultraviolet Spectrophotometric Method for the Determination of Anthracene, Naphthalene and Pyrene in Coal Tars. *J. Mol. Struct.* **1984**, *115*, 185–188. [CrossRef]
41. Abdel-Aziz, O.; El Kosasy, A.M.; El-Sayed Okeil, S.M. Comparative Study for Determination of Some Polycyclic Aromatic Hydrocarbons 'PAHs' by a New Spectrophotometric Method and Multivariate Calibration Coupled with Dispersive Liquid–Liquid Extraction. *Spectrochim. Acta A Mol. Biomol. Spectrosc.* **2014**, *133*, 119–129. [CrossRef]
42. Esteves da Silva, J.C.G.; Marques Laquipai, M.C.P.O. Method for Rapid Screening of Chlorophenols Using a Reduced Calibration Set of UV Spectra and Multivariate Calibration Techniques. *Anal. Lett.* **1998**, *31*, 2549–2563. [CrossRef]
43. Mosca Angelucci, D.; Tomei, M.C. Pentachlorophenol Aerobic Removal in a Sequential Reactor: Start-up Procedure and Kinetic Study. *Environ. Technol.* **2015**, *36*, 327–335. [CrossRef]
44. Hildebrand, J.H.; Scott, R.L. *Regular_Solutions*; Prentice-Hall, Inc.: Englewood Cliffs, NJ, USA, 1962.
45. Bacon, S.L.; Parent, J.S.; Daugulis, A.J. A Framework to Predict and Experimentally Evaluate Polymer–Solute Thermodynamic Affinity for Two-Phase Partitioning Bioreactor (TPPB) Applications. *J. Chem. Technol. Biotechnol.* **2014**, *89*, 948–956. [CrossRef]

46. Bustamante, P.; Peña, M.A.; Barra, J. The Modified Extended Hansen Method to Determine Partial Solubility Parameters of Drugs Containing a Single Hydrogen Bonding Group and Their Sodium Derivatives: Benzoic Acid/Na and Ibuprofen/Na. *Int. J. Pharm.* **2000**, *194*, 117–124. [CrossRef] [PubMed]
47. Hussain, A.; Altamimi, M.A.; Imam, S.S.; Imam, F. Green Nanoemulsion-Based Treatment to Remove Sulfamethoxazole from a Contaminated Water Solution. *J. Mol. Liq.* **2023**, *384*, 122183. [CrossRef]
48. Stapleton, M.J.; Ansari, A.J.; Hai, F.I. Antibiotic Sorption onto Microplastics in Water: A Critical Review of the Factors, Mechanisms and Implications. *Water Res.* **2023**, *233*, 119790. [CrossRef]
49. Moura, D.S.; Pestana, C.J.; Moffat, C.F.; Hui, J.; Irvine, J.T.S.; Lawton, L.A. Characterisation of Microplastics Is Key for Reliable Data Interpretation. *Chemosphere* **2023**, *331*, 138691. [CrossRef]
50. Lo, K.-H.; Anuratha, K.S.; Cheng, C.-C.; Wu, S.-J.; Juan, H.-Y.; Su, C.-H.; Lin, J.-Y.; Hsieh, C.-K. In Situ Synthesis of ZIF-67 Thin Films Using Low Temperature Chemical Vapor Deposition to Fabricate All-Solid-State Flexible Interdigital in-Planar Microsupercapacitors. *Int. J. Energy Res.* **2023**, *2023*, 3754111. [CrossRef]
51. Mosavi-Mirkolaei, S.T.; Najafi, S.K.; Tajvidi, M. Physical and Mechanical Properties of Wood-Plastic Composites Made with Microfibrillar Blends of LDPE, HDPE and PET. *Fibers Polym.* **2019**, *20*, 2156–2165. [CrossRef]
52. Liang, C.; Zheng, S.; Chen, Z.; Wei, S.; Sun, Z.; Li, C. Study on Surface Modification of Ground Calcium Carbonate with Novel Modifier and Its PVC Filling Performance. *Powder Technol.* **2022**, *412*, 118028. [CrossRef]
53. Zhou, J.; Chen, H.; Guo, Y.; Chen, Q.; Ren, H.; Tao, Y. Changes in Metal Adsorption Ability of Microplastics upon Loss of Calcium Carbonate Filler Masterbatch through Natural Aging. *Sci. Total Environ.* **2022**, *832*, 155142. [CrossRef]
54. Tummino, M.L.; Chrimatopoulos, C.; Bertolla, M.; Tonetti, C.; Sakkas, V. Configuration of a Simple Method for Different Polyamides 6.9 Recognition by ATR-FTIR Analysis Coupled with Chemometrics. *Polymers* **2023**, *15*, 3166. [CrossRef]
55. Vahur, S.; Teearu, A.; Peets, P.; Joosu, L.; Leito, I. ATR-FT-IR Spectral Collection of Conservation Materials in the Extended Region of 4000-80 Cm–1. *Anal. Bioanal. Chem.* **2016**, *408*, 3373–3379. [CrossRef]
56. Dos Santos Pereira, A.P.; Da Silva, M.H.P.; Lima, É.P.; Dos Santos Paula, A.; Tommasini, F.J. Processing and Characterization of PET Composites Reinforced with Geopolymer Concrete Waste. In *Proceedings of the Materials Research*; Universidade Federal de Sao Carlos: São Carlos, Brazil, 2017; Volume 20, pp. 411–420.
57. Chen, Z.; Hay, J.N.; Jenkins, M.J. The Thermal Analysis of Poly(Ethylene Terephthalate) by FTIR Spectroscopy. *Thermochim. Acta* **2013**, *552*, 123–130. [CrossRef]
58. Hedrick, S.A.; Chuang, S.S.C. Temperature Programmed Decomposition of Polypropylene: In Situ FTIR Coupled with Mass Spectroscopy Study. *Thermochim. Acta* **1998**, *315*, 159–168. [CrossRef]
59. Yabagi, J.A.; Kimpa, M.I.; Muhammad, M.N.; Rashid, S.B.; Zaidi, E.; Agam, M.A. The Effect of Gamma Irradiation on Chemical, Morphology and Optical Properties of Polystyrene Nanosphere at Various Exposure Time. *IOP Conf. Ser. Mater. Sci. Eng.* **2018**, *298*, 012004. [CrossRef]
60. Sabbar, A.N.; Mohammed, H.S.; Ibrahim, A.R.; Saud, H.R. Thermal and Optical Properties of Polystyrene Nanocomposites Reinforced with Soot. *Orient. J. Chem.* **2019**, *35*, 455–460. [CrossRef]
61. Beltrán, M.; Marcilla, A. Fourier transform infrared spectroscopy applied to the study of PVC decomposition. *Eur. Polym. J.* **1997**, *33*, 1135–1142. [CrossRef]
62. Smith, B. The Infrared Spectra of Polymers II: Polyethylene. *Spectroscopy* **2021**, *36*, 24–29. [CrossRef]
63. Ouyang, Z.; Zhang, Z.; Jing, Y.; Bai, L.; Zhao, M.; Hao, X.; Li, X.; Guo, X. The Photo-Aging of Polyvinyl Chloride Microplastics under Different UV Irradiations. *Gondwana Res.* **2022**, *108*, 72–80. [CrossRef]
64. Hu, Q.; Pang, S.; Wang, D. In-Depth Insights into Mathematical Characteristics, Selection Criteria and Common Mistakes of Adsorption Kinetic Models: A Critical Review. *Sep. Purif. Rev.* **2022**, *51*, 281–299. [CrossRef]
65. Zhang, X.; Liu, L.; Chen, X.; Li, J.; Chen, J.; Wang, H. The Fate and Risk of Microplastic and Antibiotic Sulfamethoxazole Coexisting in the Environment. *Environ. Geochem. Health* **2023**, *45*, 2905–2915. [CrossRef]
66. Bao, Z.Z.; Lu, S.Q.; Wang, G.; Cai, Z.; Chen, Z.F. Adsorption of 2-Hydroxynaphthalene, Naphthalene, Phenanthrene, and Pyrene by Polyvinyl Chloride Microplastics in Water and Their Bioaccessibility under in Vitro Human Gastrointestinal System. *Sci. Total Environ.* **2023**, *871*, 162157. [CrossRef]
67. Gui, B.; Xu, X.; Zhang, S.; Wang, Y.; Li, C.; Zhang, D.; Su, L.; Zhao, Y. Prediction of Organic Compounds Adsorbed by Polyethylene and Chlorinated Polyethylene Microplastics in Freshwater Using QSAR. *Environ. Res.* **2021**, *197*, 111001. [CrossRef]
68. Mejías, C.; Martín, J.; Santos, J.L.; Aparicio, I.; Alonso, E. Implications of Polystyrene and Polyamide Microplastics in the Adsorption of Sulfonamide Antibiotics and Their Metabolites in Water Matrices. *Aquat. Toxicol.* **2024**, *271*, 106934. [CrossRef]
69. Kuang, B.; Chen, X.; Zhan, J.; Zhou, L.; Zhong, D.; Wang, T. Interaction Behaviors of Sulfamethoxazole and Microplastics in Marine Condition: Focusing on the Synergistic Effects of Salinity and Temperature. *Ecotoxicol. Environ. Saf.* **2023**, *259*, 115009. [CrossRef] [PubMed]

70. Hüffer, T.; Weniger, A.-K.; Hofmann, T. Sorption of Organic Compounds by Aged Polystyrene Microplastic Particles. *Environ. Pollut.* **2018**, *236*, 218–225. [CrossRef] [PubMed]
71. Yi, X.; Bayen, S.; Kelly, B.C.; Li, X.; Zhou, Z. Improved Detection of Multiple Environmental Antibiotics through an Optimized Sample Extraction Strategy in Liquid Chromatography-Mass Spectrometry Analysis. *Anal. Bioanal. Chem.* **2015**, *407*, 9071–9083. [CrossRef] [PubMed]